Increasing Binding Constants of Ligands to Carbonic Anhydrase by Using "Greasy Tails"

Jinming Gao, Shuang Qiao, and George M. Whitesides*

Department of Chemistry, Harvard University, 12 Oxford Street, Cambridge, Massachusetts 02138

Received February 13, 1995[⊗]

Two series of *para*-substituted benzenesulfonamides have been examined as inhibitors for bovine carbonic anhydrase II (CAII, EC 4.2.1.1). Both series have hydrophobic alkyl group R connected by amide linkages to the aromatic ring ($H_2NO_2SC_6H_4$-CH_2NHCOR_1 and $H_2NO_2SC_6H_4$-$CONR_2R_3$). The free energy of partitioning (ΔG_P) of these ligands between water and octanol had similar, linear correlations with the molecular surface areas of the hydrophobic groups R; ΔG_P was only relatively weakly influenced by the linkage to the benzenesulfonamide and the detailed structure of the group R. Binding of these ligands to CAII was more complicated. For compounds having the structure $H_2NO_2SC_6H_4$-L-R, the dependence of the free energy of binding to CAII on the surface area of the hydrocarbon (fluorocarbon) group R for different -L-R was ($d\Delta G_b/dA$, kcal/(mol·100 Å^2)): -CH_2NHCOR_H, -0.71 ± 0.03; -CH_2NHCOR_F, -0.72 ± 0.07; -$CONHCH_2R_H$, -2.5 ± 0.1; and -$CONHCH_2R_F$, -2.7 ± 0.3. The available data permit several conclusions: (i) details (linear, branched, cyclic) of the structure of the group R_H are relatively unimportant in determining binding constants (although cyclic structures may bind slightly more strongly than acyclic ligands with the same carbon number); (ii) for a given class of compounds, binding constants of hydrocarbons and fluorocarbons having the same surface area are very similar; and (iii) the nature of the linker L influences the sensitivity of binding to the surface area of the group R, presumably by its influences in positioning the group in the binding pocket of the enzyme. Fluorocarbons seem to be more hydrophobic than hydrocarbons of the same carbon number because they have larger areas of hydrophobic surface; the hydrophobicity of hydrocarbon and fluorocarbon surfaces are similar, after correction for differences in area.

Introduction

The purpose of this work is to examine a strategy for increasing the strength of binding of a ligand for a protein by using hydrophobic interactions between the surface of the protein adjacent to the primary binding site and the hydrophobic residues added to the ligand (Figure 1).[1] Attachment of a hydrophobic group of appropriate size and shape—a "greasy tail"—to the ligand at a position that does not interfere with its binding would allow simultaneous interaction of the ligand with the primary binding site and of the added hydrophobic group with an adjacent, secondary, hydrophobic site on the surface of the protein. These simultaneous interactions should increase the area of the molecular surface in contact between the ligand and the protein, while retaining the specificity of the original interaction. They should therefore decrease the overall free energy of binding (ΔG_b), provided that the favorable decrease in the magnitude of ΔH_b accompanying the increase in surface area was not nullified by an unfavorable increase in free energy due to the loss in entropy of the linker as a result of bivalent binding.

This strategy has been used before—either implicitly or explicitly—in a number of instances.[2] We wish to rationalize the strategy by understanding the magnitude of the increases in binding that might be expected in a representative system of protein and ligand.

Choice of Model System. We have used a model system consisting of carbonic anhydrase II (CAII, EC 4.2.1.1)[3] and benzenesulfonamides having hydrophobic groups attached in the *para* position. This position is not in contact with the surface of the protein and points toward free solution; substituents introduced at this position change the binding affinity of benzenesulfonamide to CAII only minimally. We examined series in which the $H_2NO_2SC_6H_4$- and the hydrophobic groups R (R_1, R_2, and R_3) were connected by either -CH_2NHCO- or -CONR- (R = H, alkyl) linkages, both for synthetic convenience (some alkyl groups are available as amines,

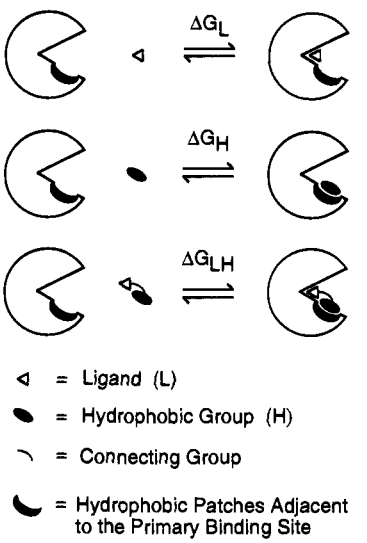

Figure 1. Strategy for increasing the binding affinity of a ligand to its receptor using nonspecific hydrophobic interactions. If ΔG_H contributes nothing to the binding, $\Delta G_{LH} \approx \Delta G_L$; if there is no entropic penalty for binding L—H, $\Delta G_{LH} \approx \Delta G_H + \Delta G_L$.

[⊗] Abstract published in *Advance ACS Abstracts*, June 1, 1995.

0022-2623/95/1838-2292$09.00/0

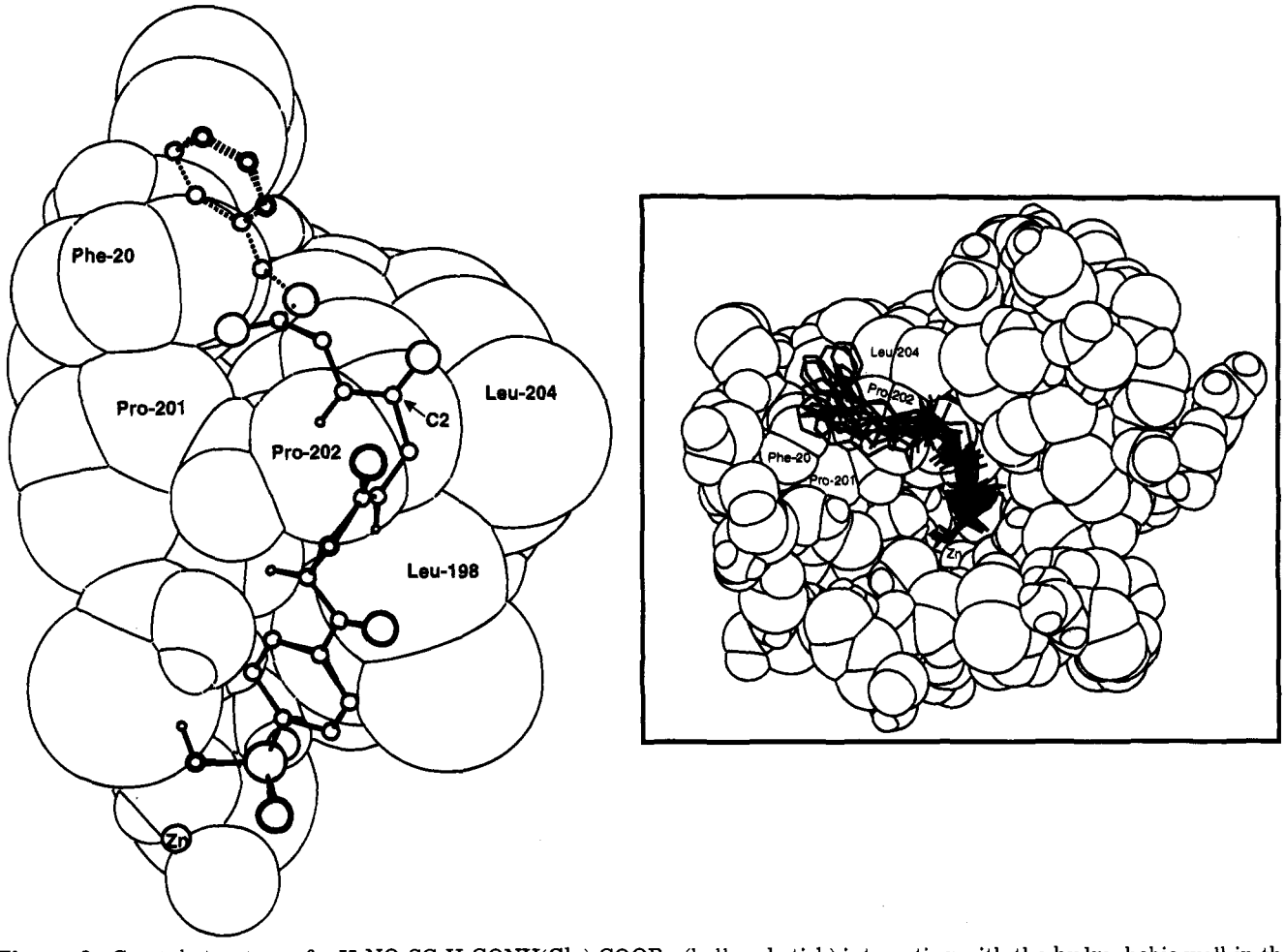

Figure 2. Crystal structure of p-$H_2NO_2SC_6H_4CONH(Gly)_3COOBn$ (ball and stick) interacting with the hydrophobic wall in the active site of HCAII (2.4 Å resolution).[7e] The hydrophobic residues of the HCAII active site are shown as van der Waals spheres. Atoms in the inhibitor that were crystallographically defined are connected by solid bonds; ill-defined atoms are connected by dashed bonds. The inset shows the simulated conformations of the inhibitors superimposed in the active site of CA using molecular dynamics.[7e]

some as carboxylic acids) and to establish the influence of these connecting groups over the behavior of groups R.

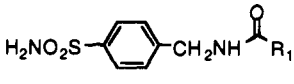

$H_2NO_2SC_6H_4$-CH_2NHCOR_1

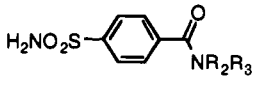

$H_2NO_2SC_6H_4$-$CONR_2R_3$

Objectives. We used CAII as the model protein in these studies for several reasons: CAII binds benzenesulfonamides in a well-defined geometry; a number of crystal structures of CAII have been reported—both with and without bound ligands—and the active site is well-defined structurally;[1a,4] carbonic anhydrases have been the subject of extensive pharmacological studies (directed toward the treatment of glaucoma[5]); CA is inexpensive and commercially available; and there are several assays for binding strengths.[6] The binding site of benzenesulfonamide is at the bottom of a conical "pit" on the surface of CAII (Figure 2): one side of the pit exposes a number of hydrophobic residues; the other side exposes primarily hydrophilic residues. Interactions directed toward these two types of surfaces can be compared from a common point of attachment to the benzenesulfonamide. A large body of data correlates structures with binding constants: some of these data[7]—especially those from Baldwin and co-workers at Merck[8] and from Christianson[1a,9]—have been accompanied by crystallographic information that detail the binding of the ligands to CAII at high resolution (<2.5 Å). This work had three objectives as follows.

(i) To establish the sensitivity of the binding affinity to the shape of the hydrophobic groups R. A reason for using the hydrophobic effect[10] as a basis for secondary interactions between ligands and their receptors is that hydrophobic interactions are relatively nondirectional.[11] In principle, a ligand with a hydrophobic tail, R, can achieve a significant increase in binding without a detailed match between the contours of the surfaces of the group R incorporated into the ligand and the hydrophobic surface of the receptor. We wished to examine the influence of the details of the shape of hydrophobic groups R on the magnitude of the additional interaction between ligand and receptor. We specifically wished to know if there was a significant opportunity to increase the strength of binding by tailoring the structure of the hydrophobic group or if the binding was insensitive to detailed structure and responded primarily to more general characteristics such as surface area.

(ii) To compare the hydrophobic effect of similar hydrocarbons and fluorocarbons in binding to CAII. Fluorocarbons are commonly considered to be "more hydrophobic" than homologous hydrocarbons.[12] Table 1 compares physical properties of hydrocarbons and

Table 1. Comparison of Physical Properties of Hydrocarbons and Fluorocarbons

physical properties	H	F	ref
Atomic Properties			
electronegativity (Pauling)	2.1	4.0	13a
covalent bond length of C-X (Å)	1.09	1.38	13b
-CX_3 Properties			
van der Waals radius (Å)	2.0	2.7	13c
molecular surface area (hemisphere, Å^2)[a]	39.4	60.6	
molecular volume (hemisphere, Å^3)[a]	16.8	42.6	
Physical Properties			
contact angle (water on poly(ethylene) or Teflon, deg)	103	112	13d
$\gamma_{X,water}$ (dynes·cm^{-1}, X = cyclohexane or Teflon)	51	50	13e
solubilities of CX_4 (mM)	1	0.1	13f
polarizability for CX_4 (10^{-24} cm^3)	2.59	3.84	13g

[a] The molecular surface area or molecular volume of -CX_3 was obtained by calculating the molecular surface area or molecular volume of CX_3CX_3 and dividing by 2.

fluorocarbons.[13] Although fluorine has been considered to be a bioisostere for hydrogen in drug design, fluorocarbons and hydrocarbons have significantly different covalent bond (C−F) lengths, van der Waals radii for -CX_3 groups, and polarizabilities. The size of fluorocarbons, as indicated by molecular surface area or molecular volume, is larger than that of hydrocarbon analogs. We wished to compare the magnitudes of changes in binding caused by adding hydrocarbons or fluorocarbons with the formulae of $R_H = C_nH_{2n+1}$ and $R_F = C_nF_{2n+1}$ to a ligand and to understand the basis of these differences.

(iii) To develop the use of molecular surface areas in estimating the magnitudes of hydrophobicities. The surface areas of molecules have been used extensively to rationalize solubilities of hydrocarbons in water,[14] to correlate with partitioning between water and organic solvent,[15] and to study the role of solvation energy in protein folding and binding.[11,16] In most cases, solvent accessible surface area (SASA)[17] has been used to estimate hydrophobic interactions. The SASA is determined from the area of the surface traced by the center of a probe sphere (e.g., 1.4 Å for water) as it is rolled over the van der Waals surface of a molecule. The molecular surface area (MSA)[18] is calculated from the area of a continuous envelope stretched over the van der Waals surface of a molecule. Although SASA and MSA are approximately proportional,[16,19] SASA is commonly used because it provides a measure of the number of water molecules that can be packed around a surface.[14c] Recently, it has been suggested that MSA is the better parameter to describe the interaction between two surfaces in contact.[15a,20] Rees et al. have suggested that solvation energies derived from crystal morphologies are better quantitated with the transfer energies between vapor and water using MSA than SASA.[20a] In this study, we chose to use the MSA of the ligands to correlate with their free energy of partitioning (ΔG_P) between octanol and water and their free energy of binding to CAII (ΔG_b).

Results and Discussion

Sensitivity of the Hydrophobic Effect to the Shapes of the Hydrophobic Tails. Table 2 and Figure 3 summarize the dependence of the hydrophobicity and binding affinity on the structure of hydrophobic groups R of compounds of the structure $H_2NO_2SC_6H_4CH_2NHCOR$ with different shapes.[21] The hydrophobicity of the ligands is represented by the partition coefficient (P) and the free energy of partition (ΔG_P) of the ligand between octanol and water phases. The partition coefficient is determined as the ratio of the concentrations of the ligand between the two phases. Figure 3A shows that the value of ΔG_P correlates linearly with the MSA of the group R. This correlation suggests that the partition coefficients are not sensitive to the details of the shape of the hydrophobic tails R and that the surface area is the predominant measure of the magnitude of hydrophobicity. The correlation gave $d\Delta G_P/dA = -2.5 \pm 0.5$ kcal/(mol·100 Å^2) (regression coefficient $r = 0.95$).[22] This value is consistent with transfer energies of 2−3 kcal/(mol·100 Å^2) for apolar compounds partitioning between a hydrocarbon-like solvent and water based on SASA.[14c,23]

Table 2. ΔG_P between Water and Octanol[a] and ΔG_b to BCA[b] for Perproteo Inhibitors p-$H_2NO_2SC_6H_4CH_2NHCOR$ with Different Shapes

ligand	R	surface area (Å^2)	partition p	partition ΔG_P (kcal/mol)	binding K_b (10^6 M^{-1})	binding ΔG_b (kcal/mol)
	C5 Inhibitors					
2A	cyclopentyl	317	6	−1.1	6.0	−9.3
2B	neopentyl	333	11	−1.4	7.1	−9.4
2C	1-ethylpropyl	334	10	−1.4	2.9	−8.8
2D	3-methylbutyl	335	11	−1.4	4.8	−9.1
2E	n-pentyl	340	17	−1.7	5.1	−9.1
	C6 Inhibitors					
2F	cyclohexyl	336	12	−1.5	7.6	−9.4
2G	cyclopentylmethyl	339	12	−1.5	6.7	−9.3
2H	2-methylpentyl	359	21	−1.8	5.7	−9.2
2I	n-hexyl	360	29	−2.0	5.7	−9.2
	C7 Inhibitors					
2J	cycloheptyl	352	31	−2.0	10.0	−9.6
2K	cyclohexylmethyl	353	42	−2.2	13.0	−9.7
2L	2,2,3,3-tetramethyl-cyclopropyl	357	37	−2.1	11.0	−9.6
2M	cyclopentylethyl	361	43	−2.2	12.0	−9.7
2N	1-ethylpentyl	379	69	−2.5	7.1	−9.4
2O	n-heptyl	383	69	−2.5	12.0	−9.7

[a] Partition coefficients were measured between octanol and 20 mM phosphate buffer (pH = 7.5). [b] Binding constants of the ligands to BCA were measured by fluorescence in 20 mM phosphate buffer (pH = 7.5).

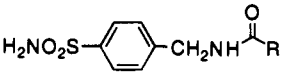

R = C_nH_{2n+1} or C_nH_{2n-1}, n = 5, 6, 7.

The free energies of binding of the ligands to CAII, ΔG_b, is dependent on the value of the pK_a of the sulfonamide group (H_2NO_2S-), hydrophobicity of the ligands, and the value of pH in the medium. In this study, ΔG_b also correlated with the surface areas of R. The correlation of ΔG_b with surface area showed slightly greater scatter than did that for ΔG_P, but the uncertainty in the measurements was also greater. The magnitude of the change in ΔG_b with area was smaller than for ΔG_P: $d\Delta G_b/dA = -0.8 \pm 0.5$ kcal/(mol·100 Å^2). Although one rationalization of this difference might be that only a fraction (30%) of the surface area of the group R contacts the hydrophobic site of the protein, results obtained with a different series of compounds ($H_2NO_2SC_6H_4CH_2NHCOR_{H/F}$) demonstrate a similar effect of surface area on partitioning and binding. Although the fractional change in surface area that we examined was small (~20%), there were no significant changes in binding constants to suggest high sensitivity

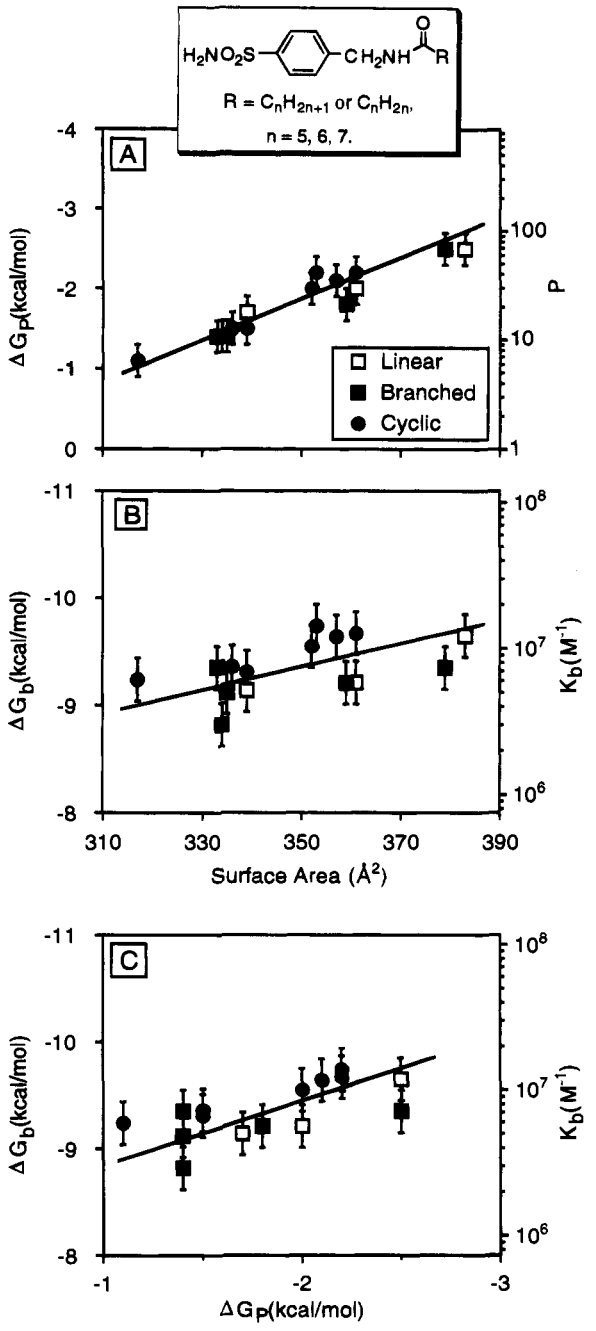

Figure 3. Values of ΔG_P of ligands p-$H_2NO_2SC_6H_4CH_2NHCOR$ between octanol and water and values of ΔG_b for binding to BCA correlate with the MSAs of ligands (A, B). The correlation between ΔG_P and ΔG_b ($d\Delta G_P/d\Delta G_b = 0.3 \pm 0.2$, $r = 0.6$[22]) suggests that hydrophobic groups with cyclic structure bind slightly more tightly to CAII than analogs having similar hydrophobicities but different geometries (C). The compounds are those given in Table 2.

of binding to details of the structure of R (Figure 3B). Figure 3C correlates the binding affinities of the ligands to their hydrophobicity. This figure suggests that cyclic structures are slightly more tightly binding to CAII than linear analogs with similar hydrophobicity. The cyclic structures might plausibly lose less entropy when binding to the surface of CAII than more conformationally mobile alkyl analogs. This qualitative hypothesis was further supported by the observation that the neopentyl side chains (**2B**) binds more tightly than less branched C_5 analogs (**2C**–**E**).

A second series of experiments examined sulfonamide ligands derived from primary and secondary amines with the same aggregate carbon numbers; these ligands

Table 3. ΔG_P between Water and Octanol[a] and ΔG_b to BCA[b] for Perproteo Inhibitors p-$H_2NO_2SC_6H_4CONR_1R_2$ with Different Dimensions

				partition		binding	
ligand	R_1	R_2	surface area (Å^2)	P	ΔG_P (kcal/mol)	K_b (10^6 M^{-1})	ΔG_b (kcal/mol)
3A	methyl	methyl	245	1.4	−0.21	11	−9.6
3B	H	ethyl	249	1.5	−0.24	5.9	−9.3
3C	ethyl	ethyl	287	8.5	−1.3	17	−9.8
3D	H	butyl	295	13	−1.5	63	−10.7
3E	propyl	propyl	332	121	−2.8	19	−9.9
3F	H	hexyl	342	163	−3.0	130	−11.0

[a] Partition coefficients were measured between octanol and 20 mM phosphate buffer (pH = 7.5). [b] Binding constants of the ligands to BCA were measured by fluorescence in 20 mM phosphate buffer (pH = 7.5).

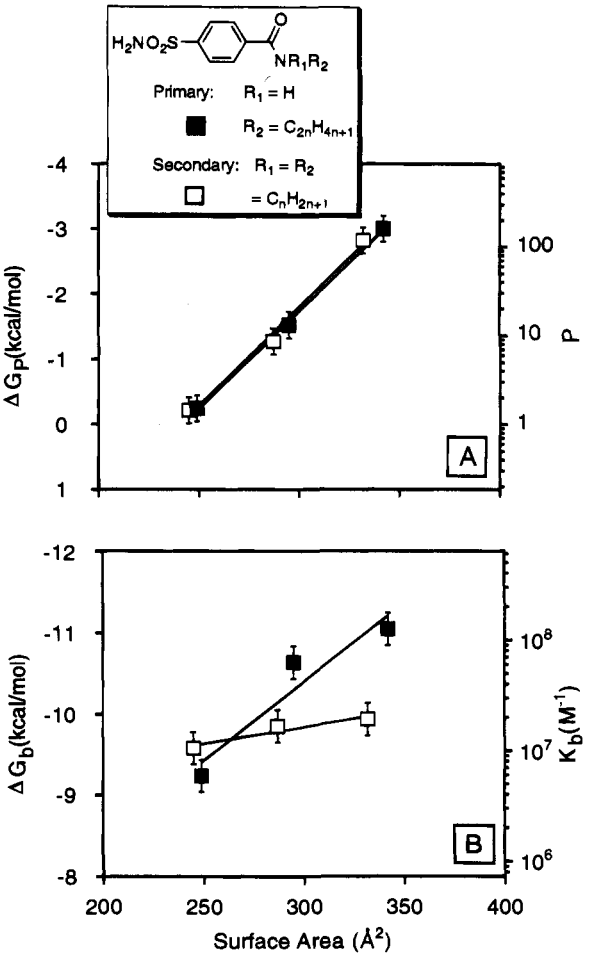

Figure 4. Dependence of ΔG_P and ΔG_b on the dimensions of inhibitors p-$H_2NO_2SC_6H_4CONR_1R_2$ (Table 3). The value of ΔG_P is correlated to MSA with similar sensitivity for both types of compounds (A): $d\Delta G_P/dA = 3.0 \pm 0.3$ kcal/(mol·100 Å^2) ($r = 0.99$). The value of ΔG_b is more sensitive to the MSA when the hydrophobic groups are disposed in one alkyl group (B): $d\Delta G_b/dA = 2.0 \pm 0.6$ kcal/(mol·100 Å^2) ($r = 0.95$); when the hydrophobic groups are disposed in two alkyl groups, $d\Delta G_b/dA = 0.5 \pm 0.1$ kcal/(mol·100 Å^2) ($r = 0.95$).

obviously have different shapes (Table 3, Figure 4).

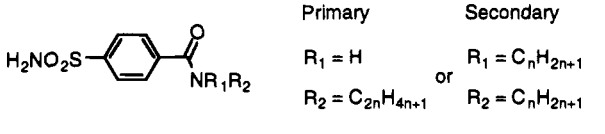

Again, in partition experiments, ΔG_P depended primarily on the MSAs and was relatively insensitive to

Table 4. ΔG_P in Water/Octanol[a] and ΔG_b to BCA[b] for Perproteo and Perfluoro Inhibitors p-$H_2NO_2SC_6H_4CH_2NHCOR$

R = -$(CH_2)_n$H						R = -$(CF_2)_n$F					
ligand	n	surface area (Å^2)	pK_a	ΔG_P (kcal/mol)	ΔG_b (kcal/mol)	ligand	n	surface area (Å^2)[c]	pK_a	ΔG_P (kcal/mol)	ΔG_b (kcal/mol)
4A	1	245	10.2	1.10	−8.5	**4G**	1	263	10.1	0.5	−9.2
4B	2	268	9.9	0.39	−8.6	**4H**	2	300	9.8	−1.4	−9.6
4C	3	291		−0.27	−8.7	**4I**	3	337		−2.1	−9.9
4D	4	314		−0.81	−8.9	**4J**	4	374		−2.7	−10.3[c]
2I	6	360		−2.0	−9.3	**4K**	6	448		−4.7	−10.7[e]
2O	7	383		−2.5	−9.4	**4L**	7	485		*d*	−10.8[e]

[a] Partition coefficients were measured between 20 mM phosphate buffer (pH = 7.5) and octanol. [b] The binding constants to BCA were measured by ACE in Tris-Gly buffer (pH = 8.3) unless otherwise indicated. [c] R = -$(CF_2)_4$H. [d] $\Delta G_P < -6$ kcal/mol. [e] The values of K_b were measured by fluorescence in Tris-Gly buffer (pH = 8.3).

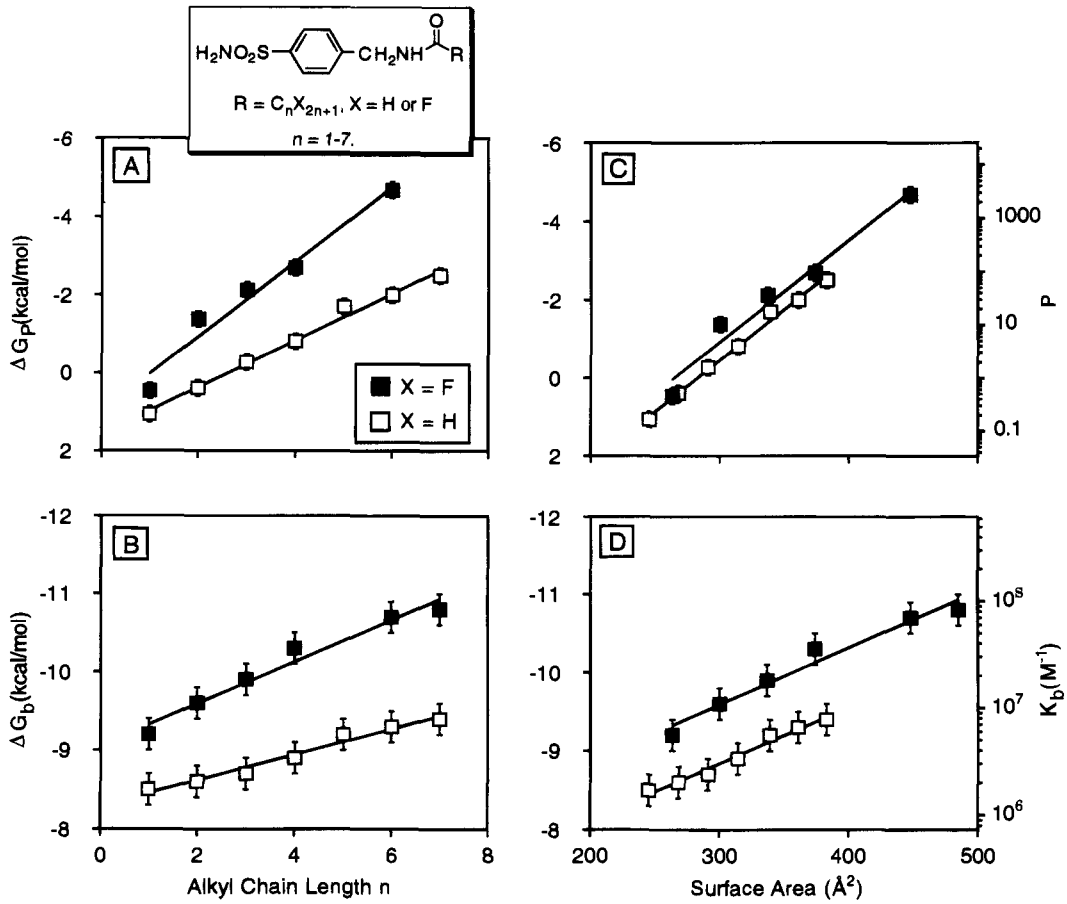

Figure 5. Dependence of the values of ΔG_P and ΔG_b of inhibitors p-$H_2NO_2SC_6H_4CH_2NHCOR$ (R = perfluoro- and perproteoalkyl chains) on their chain length and MSAs. The similar sensitivity to MSA in the two series suggests that the intrinsic hydrophobicities of fluorocarbons and hydrocarbons are the same: $d\Delta G_P/dA = -2.6 \pm 0.1$ ($r = 0.99$) and -2.6 ± 0.3 ($r = 0.98$) kcal/(mol·100 Å^2) for hydrocarbons and fluorocarbons, respectively; and $d\Delta G_b/dA = -0.71 \pm 0.03$ ($r = 0.99$) and -0.72 ± 0.07 ($r = 0.98$) kcal/mol·100 Å^2) for hydrocarbons and fluorocarbons, respectively. The observation that fluorocarbons bind to CAII slightly more strongly than hydrocarbons (as indicated from the y-intercept in panel D) with the same surface areas is probably due to a slight difference in the pK_a of the amide CON*H* hydrogens.

whether the hydrophobic surface was disposed in one or two alkyl groups (Figure 4A). Binding of these ligands to CAII depended on both their surface areas and whether the hydrocarbons were incorporated into a primary or secondary amine (Figure 4B). The reduced binding for ligands containing secondary amines compared to ligands incorporating primary amines with the same carbon number was not due to the loss of the amide NH proton—with its potential for hydrogen binding—since NHEt and NMe_2 give similar binding constants. The decreased binding of ligands with secondary amides compared to primary amides thus seems to result from the ability of the primary amide to position the longer and more flexible n-alkyl chain to contact the hydrophobic surface on the protein more effectively than that of the secondary amide with two shorter alkyl groups.

Comparison of Hydrophobicity and Its Influence on Binding for Hydrocarbons and Fluorocarbons. One of our objectives was to determine how the surface characteristics of perfluoro (fluorocarbon) or perproteo (hydrocarbon) chains affected the partitioning of the ligands between water and octanol and the binding of these ligands to CAII. In one series of ligands, we attached linear alkyl or perfluoroalkyl groups with different chain length to the aminomethyl benzenesulfonamide group (Table 4, Figure 5). Although fluorocarbons were significantly more hydrophobic than hydrocarbons of the same chain length, they showed similar intrinsic hydrophobicities (free energy of parti-

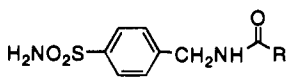

tion per unit surface area): $d\Delta G_P/dA$ ~−2.6 kcal/(mol·100 Å^2) for both hydrocarbons and fluorocarbons. Correlation of ΔG_b of the ligands to CAII with the chain length and the surface areas of the ligands gave similar trends as those of partitioning: $d\Delta G_b/dA$ was ~−0.72 kcal/(mol·100 Å^2) for both hydrocarbons and fluorocarbons. Again, the difference between $d\Delta G_P/dA$ and $d\Delta G_b/dA$ is consistent with the hypothesis that a fraction (~30%) of the hydrophobic group of the ligand contacts the surface of the protein relative to the area interacting with partitioning systems for this type of linkage (-CH_2NHCO-).

The difference between the intercepts for the sets of data for hydrocarbons and fluorocarbons in Figure 5D might, in principle, be caused by different values of the pK_a for benzenesulfonamides in each set or by enhanced hydrogen bond interactions of the amide group in the perfluoro series compared to the perproteo series. We measured the values of pK_a for the sulfonamide (H_2NO_2S) groups for four ligands: **4A**,**B**,**G**,**H**. These results showed that the length and composition of the chain—whether fluorocarbon or hydrocarbon—did not affect the value of the pK_a of the H_2NO_2S- group significantly. The differences between the values of pK_a for pairs of the same carbon number were less than 0.2 pK_a unit; this small difference (which is about the uncertainty in the measurement) cannot account for the enhancement of binding for the perfluoro series.[7a-c]

The enhancement of binding observed in the perfluoro series might also reflect stronger hydrogen bond interactions of the amide group with donors or acceptors in the active site of CAII. To test this hypothesis, since we could not measure the pK_a of the amide CON*H* directly by titration, we prepared a series of ligands in which the perfluoro group was separated from the amide by one CH_2 unit in each series (Table 5, Figure 6). The

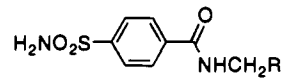

dependence of the magnitudes of ΔG_P and ΔG_b on the number of methylene units and MSAs is shown in Table 6. For these ligands, the lines correlating ΔG_b with MSAs for two series had similar intercepts (Figure 6D). Assuming again that the perfluoro group had little influence on the pK_a of the sulfonamide, this result supports the hypothesis that the intercept in the previous series reflected differences in the acidity or basicity of the amide group and resulted from the enhanced hydrogen bond interactions of this amide group with groups on the surface of the binding site of CAII.

The values of ΔG_P in this series of ligands show a sensitivity to surface area that is similar to that in the other series: $d\Delta G_P/dA$ was ~−2.8 kcal/(mol·100 Å^2) for both hydrocarbons and fluorocarbons (Table 6). This correlation indicates that partitioning is only sensitive to the surface areas of the hydrophobic tails and is not sensitive to the type of linkages. The intrinsic hydrophobicity is the same for hydrocarbons and fluorocarbons. As a comparison, ΔG_b shows significantly different sensitivity to the MSA compared to the previous series: $d\Delta G_b/dA$ was ~−2.6 kcal/(mol·100 Å^2) for both hydrocarbons and fluorocarbons (Table 6). The

Table 5. ΔG_P between Water and Octanol[a] and ΔG_b to BCA[b] for Perproteo and Perfluoro Inhibitors p-$H_2NO_2SC_6H_4CONHCH_2(CX_2)_nX$

	-$(CX_2)_n$X		surface area	partition		binding	
ligand	X	n	(Å^2)	P	ΔG_P (kcal/mol)	K_b (10^6 M^{-1})	ΔG_b (kcal/mol)
3B	H	1	249	1.5	−0.24	5.9	−9.3
5A	F	1	270	7.0	−1.1	47	−10.5
5B	H	2	271	3.4	−0.71	26	−10.1
5C	F	2	303	33	−2.1	180	−11.3
3D	H	3	295	13	−1.5	63	−10.7
5D	F	3	333	110	−2.8	1100	−12.3

[a] Partition coefficients were measured between octanol and 20 mM phosphate buffer (pH = 7.5). [b] Binding constants of the ligands to BCA were measured by fluorescence in 20 mM phosphate buffer (pH = 7.5).

different sensitivity of ΔG_b to surface area in the two series having different linkages (Table 6) indicates two possibilities of hydrophobic interaction: different hydrophobic sites on CAII interact with hydrophobic groups from different linkages or the same hydrophobic site on CAII interacts with the hydrophobic groups from the two series with different degrees of contact. X-ray crystallographic studies of the complex structure of representative ligands with CAII may be able to distinguish between these two possibilities.

Conclusion

The magnitude of the binding of *para*-substituted benzenesulfonamide ($H_2NO_2SC_6H_4$-CH_2NHCOR_1 and -$CONR_2R_3$) to CAII is determined predominantly by the surface area of the hydrophobic group R, by the connecting group (-CH_2NHCO- or -CONR-), and not by the details of the structure of the hydrophobic group. We observed only small systematic differences, at the border of observability, among different types of alkyl groups, with cyclic compounds binding slightly more tightly than linear or branched analogs. These results support the idea that hydrophobic bonding to the surface of CAII is relatively insensitive to the structure of the alkyl group.

The free energy of partitioning (ΔG_P) seems to be determined primarily by the MSAs of the ligands and is independent of the groups connecting them to the benzenesulfonamide moiety. By contrast, the free energy of binding (ΔG_b) depends on the type of connecting groups: $d\Delta G_b/100$ Å^2 ≈ −0.72 kcal/(mol·100 Å^2) for compounds containing the -CH_2NHCO- linkage, and $d\Delta G_b/100$ Å^2 ≈ −2.6 kcal/(mol·100 Å^2) for those having the -$CONHCH_2$- linkage. These results suggest the hydrophobic groups having different linkages to benzenesulfonamide either interact with different hydrophobic sites on the CAII or interact with the same hydrophobic site with different degrees of contact (Table 6).

Comparison of hydrocarbons and fluorocarbons in partition experiments showed that their intrinsic hydrophobicities are the same: $d\Delta G_P/100$ Å^2 ≈ −2.7 kcal/(mol·100 Å^2); fluorocarbons are more hydrophobic than hydrocarbons of the same carbon number because they have larger surface areas. The similarity between hydrocarbons and fluorocarbons may be useful in designing inhibitors based on hydrophobic effect. The properties of the two classes of compounds are predicted to be similar (for similar surface areas); the fluorocarbons should, however, be more resistant to oxidative metabolism than the hydrocarbons.

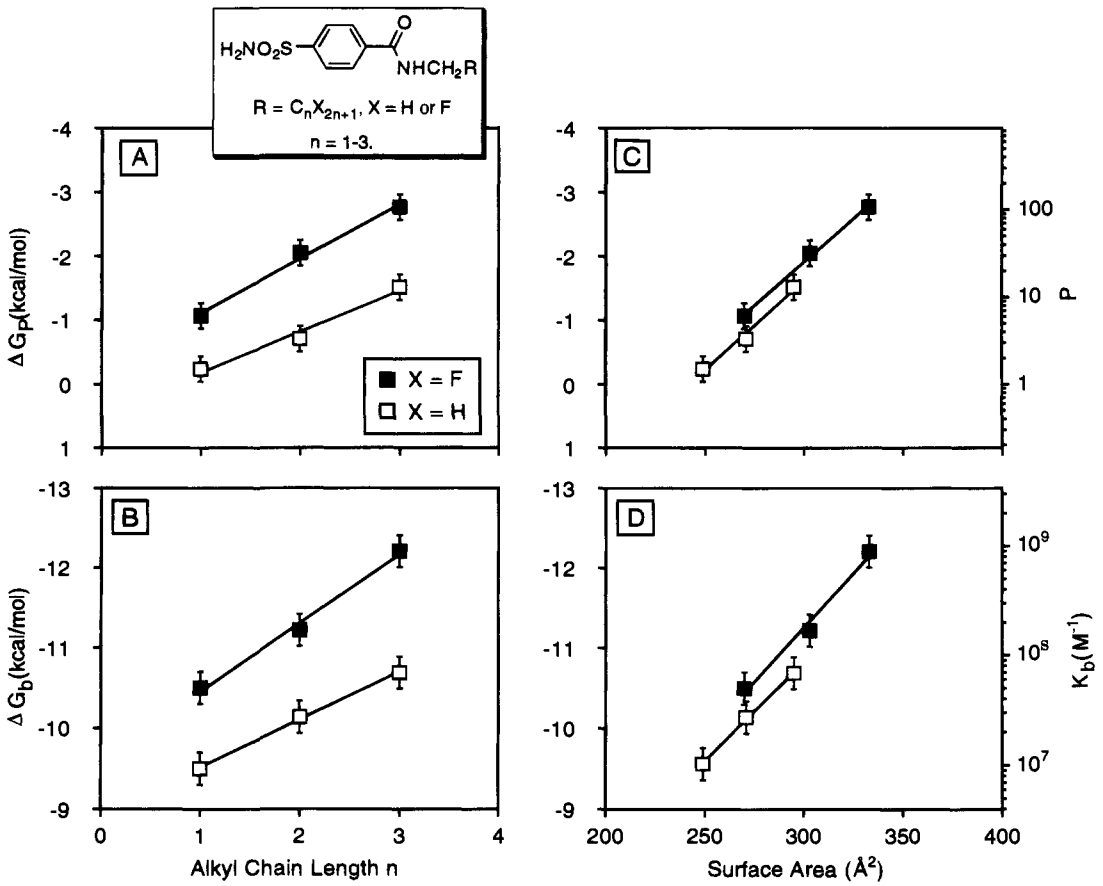

Figure 6. Values of ΔG_P for partitioning between octanol and water, and values of ΔG_b for binding to CAII correlated with MSA for compounds with structure p-$H_2NO_2SC_6H_4CONHCH_2R$. The similar sensitivity to MSA from two series suggests that both the intrinsic hydrophobicities and the strength of binding of fluorocarbons and hydrocarbons of the same surface area are the same: $d\Delta G_P/dA = -2.8 \pm 0.1$ ($r = 0.99$) and -2.7 ± 0.1 ($r = 0.99$) kcal/(mol·100 Å^2) for hydrocarbons and fluorocarbons, respectively; and $d\Delta G_b/dA = -2.5 \pm 0.1$ ($r = 0.99$) and -2.7 ± 0.3 ($r = 0.99$) kcal/(mol·100 Å^2) for hydrocarbons and fluorocarbons, respectively.

Table 6. Dependence of Magnitudes of ΔG_P[a] and ΔG_b[b] on the Number of Methylene Units and MSAs

ligands	type: NH_2O_2SAr-	$\Delta G_P/CX_2$ (kcal/mol)	ΔG_P/100 Å^2 (kcal/(mol·100 Å^2))	$\Delta G_b/CX_2$ (kcal/mol)	ΔG_b/100 Å^2 (kcal/(mol·100 Å^2))
4A–D, 2I, O	$-CH_2NHCOR_H$	-0.60 ± 0.03[c]	-2.6 ± 0.1	-0.16 ± 0.01[d]	-0.71 ± 0.03
4G–L	$-CH_2NHCOR_F$	-0.9 ± 0.1[e]	-2.6 ± 0.3	-0.27 ± 0.03[f]	-0.72 ± 0.07
3B,D, 5B	$-CONHCH_2R_H$	-0.64 ± 0.03[g]	-2.8 ± 0.1	-0.56 ± 0.01[h]	-2.5 ± 0.1
5A,C,D	$-CONHCH_2R_F$	-0.85 ± 0.02[i]	-2.7 ± 0.1	-0.86 ± 0.05[j]	-2.7 ± 0.3
3A,C,E	-CONRR		-3.0 ± 0.3		-0.5 ± 0.1

[a] Partition coefficients were measured between 20 mM phosphate buffer (pH = 7.5) and octanol. [b] The dissociation constants to BCA were measured by ACE in 25 mM Tris and 192 mM Gly buffer (pH = 8.3) or by fluorescence in 20 mM phosphate buffer (pH = 7.5). [c] $r = 0.99$. [d] $r = 0.99$. [e] $r = 0.98$. [f] $r = 0.98$. [g] $r = 0.99$. [h] $r = 0.99$. [i] $r = 0.99$. [j] $r = 0.99$.

In summary, this paper suggests that hydrophobic surface area, rather than details of the structure of the hydrophobic group, is the dominant factor in determining the strength of hydrophobic binding to the hydrophobic surface of CAII. We observed a maximum enhancement in binding of 2.6 kcal/(mol·100 Å^2) from interactions between hydrophobic surfaces. Fluorocarbons are similar to hydrocarbons in their hydrophobic binding, although they may differ in their influence on polar interactions.

Experimental Section

Calculation of the SASAs and MSAs. The Quanta 3.3 parameter set from Molecular Simulation Inc. and the CHARMm 22 molecular mechanics program were used for the computations in this study.[24] We built the structure of the ligands using standard valence geometries in Quanta 3.3 and used it as the starting conformations for energy minimizations. The conformational energy was minimized using adopted-basis Newton–Raphson (ABNR) until the gradient in the potential energies reached 0.01 kcal/mol/Å. We assume that this conformation represents the average conformations of the ligand in both binding and partitioning experiments. We used the above conformation and van der Waals radii to calculate the MSAs of the ligands. The SASAs were calculated similarly, except that another probe radius (1.4 Å) was added to each van der Waals radius used for the calculation of the MSAs.

Synthesis of Derivatives of Benzenesulfonamides. Synthesis of the two types of sulfonamide ligands followed literature procedures.[6c]

2A: ^{1}H NMR (400 MHz, DMSO-d_6) δ 8.25 (t, $J = 5.8$ Hz, 1 H), 7.64 (d, $J = 8.2$ Hz, 2 H), 7.27 (d, $J = 8.2$ Hz, 2 H), 7.18 (s, 2 H), 4.19 (d, $J = 5.9$ Hz, 2 H), 1.68–1.37 (m, 9 H); ^{13}C NMR (100 MHz, DMSO-d_6) δ 175.43, 144.00, 142.51, 127.35, 125.67, 44.28, 41.28, 29.96, 25.60; HRMS (M^+) calcd for $C_{13}H_{18}N_2O_3S$ 282.3600, found 282.1038.

2B: ^{1}H NMR (400 MHz, DMSO-d_6) δ 8.36 (t, $J = 5.8$ Hz, 1 H), 7.75 (d, $J = 7.8$ Hz, 2 H), 7.41 (d, $J = 8.0$ Hz, 2 H), 7.31 (s, 2 H), 4.30 (d, $J = 5.9$ Hz, 2 H), 2.02 (s, 2 H), 0.95 (s, 9 H); ^{13}C NMR (100 MHz, DMSO-d_6) δ 171.99, 144.83, 128.35, 126.39,

48.99, 41.90, 30.68, 29.87; HRMS (M + H)$^+$ calcd for $C_{13}H_{20}N_2O_3S$ 285.1273, found 285.1273. Anal. ($C_{13}H_{20}N_2O_3S$) C, H, N.

2C: ^{1}H NMR (400 MHz, DMSO-d_6) δ 8.43 (t, J = 5.9 Hz, 1 H), 7.76 (d, J = 8.3 Hz, 2 H), 7.42 (d, J = 8.3 Hz, 2 H), 7.30 (s, 2 H), 4.34 (d, J = 6.0 Hz, 2 H), 2.06–1.99 (m, 1 H), 1.53–1.31 (m, 4 H), 0.79 (t, J = 7.4 Hz, 6 H); ^{13}C NMR (100 MHz, DMSO-d_6) δ 174.84, 144.07, 142.53, 127.47, 125.61, 49.18, 41.61, 25.22, 11.90; HRMS (M + H)$^+$ calcd for $C_{13}H_{20}N_2O_3S$ 285.1273, found 258.1273.

2D: ^{1}H NMR (400 MHz, DMSO-d_6) δ 8.40 (t, J = 5.8 Hz, 1 H), 7.75 (d, J = 8.4 Hz, 2 H), 7.39 (d, J = 8.4 Hz, 2 H), 7.28 (s, 2 H), 4.30 (d, J = 5.9 Hz, 2 H), 2.16–2.12 (m, 2 H), 1.51–1.38 (m, 5 H), 0.86–0.82 (m, 6 H); ^{13}C NMR (100 MHz, DMSO-d_6) δ 172.41, 143.84, 142.52, 127.38, 125.61, 41.62, 34.24, 33.36, 27.19, 22.21; HRMS (M + H)$^+$ calcd for $C_{13}H_{20}N_2O_3S$ 285.1273, found 285.1273.

2E: ^{1}H NMR (400 MHz, DMSO-d_6) δ 8.37 (t, J = 6.0 Hz, 1 H), 7.75 (d, J = 8.2 Hz, 2 H), 7.39 (d, J = 8.1 Hz, 2 H), 7.29 (s, 2 H), 4.30 (d, J = 6.0 Hz, 2 H), 2.13 (t, J = 7.5 Hz, 2 H), 1.52 (t, J = 7.3 Hz, 2 H), 1.25 (m, 4 H), 0.85 (t, J = 7.0 Hz, 3 H); ^{13}C NMR (100 MHz, DMSO-d_6) δ 172.30, 143.87, 142.52, 127.40, 125.61, 41.61, 35.25, 30.87, 24.90, 21.80, 7.29; HRMS (M + H)$^+$ calcd for $C_{13}H_{20}N_2O_3S$ 285.1273, found 285.1273.

2F: ^{1}H NMR (400 MHz, DMSO-d_6) δ 8.33 (t, J = 5.8 Hz, 1 H), 7.75 (d, J = 8.2 Hz, 2 H), 7.38 (d, J = 8.2 Hz, 2 H), 7.31 (s, 2 H), 4.29 (d, J = 5.9 Hz, 2 H), 2.19–2.13 (m, 1 H), 1.72–1.12 (m, 10 H); ^{13}C NMR (100 MHz, DMSO-d_6) δ 175.29, 144.01, 142.48, 127.25, 125.63, 43.94, 41.46, 29.20, 25.44, 25.25; HRMS (M + H)$^+$ calcd for $C_{14}H_{20}N_2O_3S$ 297.3951, found 297.1273. Anal. ($C_{14}H_{20}N_2O_3S$) C, H, N.

2G: ^{1}H NMR (400 MHz, DMSO-d_6) δ 8.38 (t, J = 5.9 Hz, 1 H), 7.74 (d, J = 8.4 Hz, 2 H), 7.39 (d, J = 8.2 Hz, 2 H), 7.30 (s, 2 H), 4.30 (d, J = 5.9 Hz, 2 H), 2.12–2.15 (m, 3 H), 1.69–1.67 (m, 2 H), 1.58–1.45 (m, 4 H), 1.14–1.09 (m, 2 H); ^{13}C NMR (100 MHz, DMSO-d_6) δ 171.87, 143.94, 142.52, 127.40, 125.68, 44.94, 41.56, 36.66, 31.90, 24.50; HRMS (M + H)$^+$ calcd for $C_{14}H_{20}N_2O_3S$ 297.3951, found 297.1273.

2H: ^{1}H NMR (400 MHz, DMSO-d_6) δ 8.38 (t, J = 5.6 Hz, 1 H), 7.76 (d, J = 8.2 Hz, 2 H), 7.39 (d, J = 8.2 Hz, 2 H), 7.30 (s, 2 H), 4.31 (m, 2 H), 2.29 (m, 1 H), 1.51–1.12 (m, 6 H), 1.04 (d, J = 6.8 Hz, 3 H), 0.84 (t, J = 8.2 Hz, 3 H); ^{13}C NMR (100 MHz, DMSO-d_6) δ 175.75, 143.99, 142.52, 127.32, 125.61, 41.52, 38.65, 33.47, 29.13, 22.07, 17.97, 13.85; HRMS (M + H)$^+$ calcd for $C_{14}H_{22}N_2O_3S$ 299.4110, found 299.1429.

2I: ^{1}H NMR (400 MHz, DMSO-d_6) δ 8.38 (t, J = 5.9 Hz, 1 H), 7.75 (d, J = 8.4 Hz, 2 H), 7.39 (d, J = 8.4 Hz, 2 H), 7.30 (s, 2 H), 4.30 (d, J = 5.9 Hz, 2 H), 2.13 (t, J = 7.4 Hz, 2 H), 1.52–1.24 (m, 8 H), 0.87 (t, J = 6.0 Hz, 3 H); ^{13}C NMR (100 MHz, DMSO-d_6) δ 172.33, 143.93, 142.55, 127.43, 125.66, 41.64, 35.33, 31.01, 28.35, 25.23, 22.03, 13.95; HRMS (M$^+$) calcd for $C_{14}H_{22}N_2O_3S$ 298.4030, found 298.1351. Anal. ($C_{14}H_{22}N_2O_3S$) C, H, N.

2J: ^{1}H NMR (400 MHz, DMSO-d_6) δ 8.30 (t, J = 5.9 Hz, 1 H), 7.75 (d, J = 8.5 Hz, 2 H), 7.37 (d, J = 8.3 Hz, 2 H), 7.30 (s, 2 H), 4.27 (d, J = 5.9 Hz, 2 H), 2.31 (m, 1 H), 1.76–1.41 (m, 12 H); ^{13}C NMR (100 MHz, DMSO-d_6) δ 176.23, 144.58, 142.98, 127.29, 125.62, 45.55, 41.45, 31.12, 27.84, 26.08; HRMS (M + H)$^+$ calcd for $C_{15}H_{22}N_2O_3S$ 311.4222, found 311.1429.

2K: ^{1}H NMR (500 MHz, DMSO-d_6) δ 8.38 (t, J = 5.9 Hz, 1 H), 7.75 (d, J = 8.2 Hz, 2 H), 7.39 (d, J = 8.2 Hz, 2 H), 7.29 (s, 2 H), 4.30 (d, J = 5.9 Hz, 2 H), 2.02 (d, J = 7.0 Hz, 2 H), 1.63 (m, 6 H), 1.23–1.05 (m, 3 H), 0.95–0.85 (m, 2 H); ^{13}C NMR (125 MHz, DMSO-d_6) δ 171.44, 143.89, 142.51, 127.39, 125.60, 43.17, 41.60, 34.63, 32.51, 25.81, 25.56; HRMS (M + H)$^+$ calcd for $C_{15}H_{22}N_2O_3S$ 311.4222, found 311.1429.

2L: ^{1}H NMR (400 MHz, DMSO-d_6) δ 8.35 (t, J = 5.9 Hz, 1 H), 7.73 (d, J = 8.4 Hz, 2 H), 7.38 (d, J = 8.4 Hz, 2 H), 7.29 (s, 2 H), 4.28 (d, J = 5.9 Hz, 2 H), 3.33 (s, 1 H), 1.16 (s, 6 H), 1.11 (s, 6 H); ^{13}C NMR (100 MHz, DMSO-d_6) δ 171.87, 144.99, 143.24, 128.14, 126.39, 41.91, 36.16, 27.22, 23.69, 16.76; HRMS (M + H)$^+$ calcd for $C_{15}H_{22}N_2O_3S$ 311.4222, found 311.1429.

2M: ^{1}H NMR (400 MHz, DMSO-d_6) δ 8.390 (t, J = 5.9 Hz, 1 H), 7.74 (d, J = 8.4 Hz, 2 H), 7.38 (d, J = 8.4 Hz, 2 H), 7.30 (s, 2 H), 4.29 (d, J = 5.9 Hz, 2 H), 2.14 (t, J = 7.5 Hz, 2 H), 1.72–1.44 (m, 9 H), 1.04 Im, 2 H); ^{13}C NMR (100 MHz, DMSO-d_6) δ 173.31, 144.68, 143.30, 128.12, 126.39, 41.84, 34.88, 32.18, 31.72, 24.80, 22.85; HRMS (M + H)$^+$ calcd for $C_{15}H_{22}N_2O_3S$ 311.4222, found 311.1429.

2N: ^{1}H NMR (400 MHz, DMSO-d_6) δ 8.44 (t, J = 5.9 Hz, 1 H), 7.75 (d, J = 8.4 Hz, 2 H), 7.40 (d, J = 8.4 Hz, 2 H), 7.31 (s, 2 H), 4.32 (d, J = 5.9 Hz, 2 H), 2.08 (m, 1 H), 1.50–1.15 (m, 8 H), 0.80 (m, 6 H); ^{13}C NMR (100 MHz, DMSO-d_6) δ 174.98, 144.11, 142.56, 127.47, 125.62, 47.42, 41.59, 32.01, 29.32, 25.67, 22.15, 13.95, 11.98; HRMS (M + H)$^+$ calcd for $C_{15}H_{24}N_2O_3S$ 313.4381, found 313.1586.

2O: ^{1}H NMR (400 MHz, DMSO-d_6) δ 8.44 (t, J = 5.9 Hz, 1 H), 7.74 (d, J = 8.4 Hz, 2 H), 7.38 (d, J = 8.4 Hz, 2H), 7.31 (s, 2 H), 4.30 (d, J = 5.9 Hz, 2 H), 2.11 (t, J = 7.5 Hz, 2 H), 1.50 (m, 2 H), 1.23 (m, 8 H), 0.83 (t, J = 7.1 Hz, 3 H); ^{13}C NMR (100 MHz, DMSO-d_6) δ 172.26, 143.89, 142.53, 127.39, 125.43, 41.60, 35.28, 31.15, 28.60, 28.39, 25.23, 22.08, 13.98; HRMS (M + H)$^+$ calcd for $C_{15}H_{24}N_2O_3S$ 313.4381, found 313.1586.

3A: ^{1}H NMR (400 MHz, DMSO-d_6) δ 7.88 (d, J = 8.1 Hz, 2 H), 7.59 (d, J = 8.1 Hz, 2 H), 7.46 (s, 2 H), 2.99 (s, 3 H), 2.87 (s, 3 H); ^{13}C NMR (100 MHz, DMSO-d_6) δ 168.98, 144.63, 139.76, 127.50, 125.75, 38.86, 34.75; HRMS (M + H)$^+$ calcd for $C_9H_{12}N_2O_3S$ 229.2756, found 229.0647.

3C: ^{1}H NMR (400 MHz, DMSO-d_6) δ 7.87 (d, J = 8.1 Hz, 2 H), 7.53 (d, J = 8.0 Hz, 2 H), 7.44 (s, 2 H), 3.43 (m, 2 H), 3.13 (m, 2 H), 1.14 (s, 3 H), 1.03 (s, 3 H); ^{13}C NMR (100 MHz, DMSO-d_6) δ 168.76, 144.32, 140.47, 126.64, 125.85, 42.80, 38.75, 13.93, 12.78; HRMS (M + H)$^+$ calcd for $C_{11}H_{16}N_2O_3S$ 257.3297, found 257.0960.

3E: ^{1}H NMR (400 MHz, DMSO-d_6) δ 7.87 (d, J = 8.3 Hz, 2 H), 7.51 (d, J = 8.3 Hz, 2 H), 7.45 (s, 2 H), 3.37 (t, J = 7.1 Hz, 2 H), 3.07 (t, J = 7.1 Hz, 2 H), 1.60 (m, 2 H), 1.46 (m, 2 H), 0.90 (t, J = 7.2 Hz, 3 H), 0.65 (t, J = 7.2 Hz, 3 H); ^{13}C NMR (100 MHz, DMSO-d_6) δ 169.30, 144.28, 140.54, 126.83, 125.89, 49.95, 45.64, 21.29, 20.28, 11.25, 10.83; HRMS (M + H)$^+$ calcd for $C_{13}H_{20}N_2O_3S$ 285.1273, found 285.1273.

4A: ^{1}H NMR (400 MHz, DMSO-d_6) δ 8.43 (t, J = 5.6 Hz, 1 H), 7.75 (d, J = 8.2 Hz, 2 H), 7.40 (d, J = 8.2 Hz, 2 H), 7.30 (s, 2 H), 4.28 (d, J = 6.0 Hz, 2 H), 1.67 (s, 3 H); ^{13}C NMR (100 MHz, DMSO-d_6) δ 169.50, 143.81, 142.60, 127.59, 125.74, 41.82, 22.60; HRMS (M + H)$^+$ calcd for $C_9H_{12}N_2O_3S$ 228.0569, found 228.0565. Anal. ($C_9H_{12}N_2O_3S$) C, H, N.

4B: ^{1}H NMR (400 MHz, DMSO-d_6) δ 8.37 (t, J = 5.9 Hz, 1 H), 7.75 (d, J = 8.1 Hz, 2 H), 7.40 (d, J = 8.3 Hz, 2 H), 7.31 (s, 2 H), 4.30 (d, J = 6.0 Hz, 2 H), 2.14 (q, J = 7.6 Hz, 2 H), 1.01 (t, J = 7.6 Hz, 3 H); ^{13}C NMR (100 MHz, DMSO-d_6) δ 173.06, 143.90, 142.54, 127.48, 125.69, 41.65, 28.46, 9.94; HRMS (M + H)$^+$ calcd for $C_{10}H_{14}N_2O_3S$ 243.0803, found 243.0798.

4C: ^{1}H NMR (400 MHz, DMSO-d_6) δ 8.49 (t, J = 5.9 Hz, 1 H), 7.74 (d, J = 8.3 Hz, 2 H), 7.39 (d, J = 8.1 Hz, 2 H), 7.31 (s, 2 H), 4.30 (d, J = 6.0 Hz, 2 H), 2.11 (t, J = 7.2 Hz, 2 H), 1.53 (m, 2 H), 0.85 (t, J = 7.4 Hz, 3 H); ^{13}C NMR (100 MHz, DMSO-d_6) δ 172.35, 143.99, 142.60, 127.53, 125.75, 41.72, 18.77, 13.73; HRMS (M)$^+$ calcd for $C_{11}H_{16}N_2O_3S$ 256.0882, found 256.0888.

4D: ^{1}H NMR (400 MHz, DMSO-d_6) δ 8.39 (t, J = 5.9 Hz, 1 H), 7.74 (d, J = 8.2 Hz, 2 H), 7.38 (d, J = 8.2 Hz, 2 H), 7.30 (s, 2 H), 4.29 (d, J = 6.0 Hz, 2 H), 2.13 (t, J = 7.3 Hz, 2 H), 1.49 (m, 2 H), 1.27 (m, 2 H), 0.86 (t, J = 7.4 Hz, 3 H); ^{13}C NMR (100 MHz, DMSO-d_6) δ 172.44, 143.96, 142.58, 127.49, 125.73, 41.71, 35.11, 27.49, 21.90, 13.79; HRMS (M + H)$^+$ calcd for $C_{12}H_{18}N_2O_3S$ 271.111, found 271.112.

4G: ^{1}H NMR (400 MHz, DMSO-d_6) δ 10.10 (t, J = 5.7 Hz, 1 H), 7.81 (d, J = 8.3 Hz, 2 H), 7.45 (d, J = 8.3 Hz, 2 H), 7.35 (s, 2 H), 4.45 (d, J = 5.9 Hz, 2 H); ^{13}C NMR (100 MHz, DMSO-d_6) δ 156.50, 143.18, 141.47, 127.84, 125.98, 42.30; HRMS (M)$^+$ calcd for $C_9H_9F_3N_2O_3S$ 282.0286, found 282.0287.

4H: ^{1}H NMR (400 MHz, DMSO-d_6) δ 10.17 (s, 1 H), 7.81 (d, J = 8.3 Hz, 2 H), 7.42 (d, J = 8.3 Hz, 2 H), 7.34 (s, 2 H), 4.47 (s, 2 H); ^{13}C NMR (100 MHz, DMSO-d_6) δ 157.09, 143.20, 141.50, 127.74, 125.99, 42.43; HRMS (M + H)$^+$ calcd for $C_{10}H_9F_5N_2O_3S$ 333.0332, found 333.0337.

4I: ^{1}H NMR (400 MHz, DMSO-d_6) δ 10.20 (s, 1 H), 7.81 (d, J = 8.1 Hz, 2 H), 7.44 (d, J = 8.2 Hz, 2 H), 7.36 (s, 2 H), 4.49 (s, 2 H); ^{13}C NMR (100 MHz, DMSO-d_6) δ 157.00, 143.29, 141.55, 127.86, 126.04, 42.64; HRMS (M)$^+$ calcd for $C_{11}H_9F_7N_2O_3S$ 382.022, found 382.023.

4J: ^{1}H NMR (400 MHz, DMSO-d_6) δ 10.10 (s, 1 H), 7.78 (d, J = 8.3 Hz, 2 H), 7.42 (d, J = 8.3 Hz, 2 H), 7.34 (s, 2 H), 7.06 (tt, J = 50.3, 5.6 Hz, 1 H), 4.46 (s, 2 H); ^{13}C NMR (100 MHz,

DMSO-d_6) δ 156.87, 143.15, 141.41, 127.71, 125.94, 42.50; HRMS (M + H)$^+$ calcd for $C_{12}H_{10}F_8N_2O_3S$ 415.0363, found 415.0355.

4K: ^{1}H NMR (400 MHz, DMSO-d_6) δ 10.20 (s, 1 H), 7.81 (d, J = 8.2 Hz, 2 H), 7.45 (d, J = 8.4 Hz, 2 H), 7.37 (s, 2 H), 4.49 (s, 2 H); ^{13}C NMR (100 MHz, DMSO-d_6) δ 157.02, 143.31, 141.56, 127.87, 126.05, 42.64; HRMS (M)$^+$ calcd for $C_{14}H_9F_{13}N_2O_3S$ 532.012, found 532.011.

4L: ^{1}H NMR (400 MHz, DMSO-d_6) δ 10.21 (s, 1 H), 7.80 (d, J = 8.3 Hz, 2 H), 7.42 (d, J = 8.1 Hz, 2 H), 7.35 (s, 2 H), 4.47 (s, 2 H); ^{13}C NMR (100 MHz, DMSO-d_6) δ 157.01, 143.30, 141.56, 127.87, 126.04, 42.64; HRMS (M)$^+$ calcd for $C_{15}H_9F_{15}N_2O_3S$ 582.009, found 582.008.

5A: ^{1}H NMR (400 MHz, DMSO-d_6) δ 9.29 (t, J = 6.1 Hz, 1 H), 8.02 (d, J = 8.1 Hz, 2 H), 7.93 (d, J = 8.0 Hz, 2 H), 7.51 (s, 2 H), 4.11 (m, 2 H); ^{13}C NMR (100 MHz, DMSO-d_6) δ 166.02, 146.83, 136.10, 128.19, 125.79, 40.42; HRMS (M)$^+$ calcd for $C_9H_9F_3N_2O_3S$ 282.028, found 282.026.

5C: ^{1}H NMR (400 MHz, DMSO-d_6) δ 9.28 (t, J = 6.1 Hz, 1 H), 8.02 (d, J = 7.9 Hz, 2 H), 7.93 (d, J = 7.8 Hz, 2 H), 7.51 (s, 2 H), 4.17 (m, 2 H); ^{13}C NMR (100 MHz, DMSO-d_6) δ 152.46, 133.06, 122.18, 114.25, 111.88, 23.94; HRMS (M + H)$^+$ calcd for $C_{10}H_9F_5N_2O_3S$ 333.0332, found 333.0318.

5D: ^{1}H NMR (400 MHz, DMSO-d_6) δ 9.26 (s, 1 H), 8.03 (d, J = 8.1 Hz, 2 H), 7.94 (d, J = 8.0 Hz, 2 H), 7.51 (s, 2 H), 4.19 (m, 2 H); ^{13}C NMR (100 MHz, DMSO-d_6) δ 152.54, 133.07, 122.20, 114.26, 111.88, 24.06; HRMS (M + H)$^+$ calcd for $C_{11}H_9F_7N_2O_3S$ 383.030, found 383.032.

Measurement of Partition Coefficients. Partition coefficients, P, of the ligands between octanol and 20 mM sodium phosphate buffer (pH = 7.5) were measured at 20 °C (eq 1).

$$P = \frac{C_{oct}}{C_w} = \left(\frac{C_oV_o - C_wV_w}{V_{oct}}\right)\frac{1}{C_w} \quad (1)$$

$$P = \frac{C_{oct}}{C_w} = e^{-\Delta G_P/RT} \quad (2)$$

The octanol and buffered aqueous solutions were presaturated by each other before use. A saturated solution of the ligand in 20 mM sodium phosphate buffer (pH = 7.5) was first prepared, and its concentration was measured by UV (C_o). The ligand in a volume (V_o) of this solution was partitioned between the water and octanol phases in a 20 °C water bath for 24 h. The ratio of the volume of the two phases (V_o vs V_w) was adjusted inversely proportional to the partition coefficient crudely measured initially so that the ligand could partition in the above two phases equally. The concentration of a ligand in the aqueous phase (C_2) was measured by UV absorption; its concentration in octanol (C_{oct}) was calculated by the difference between the total amount of ligand (C_oV_o) and the amount of ligand in water (C_wV_w) divided by the volume of octanol (V_{oct}).[25] The observed range of variation in the partition coefficients between 20 and 70 °C was small; the insensitivity of the partition coefficients to temperature[26] prevented the determination of enthalpic and entropic contributions to ΔG_P.

Measurement of Binding Constants. Both fluorescence spectroscopy[6c] and affinity capillary electrophoresis (ACE)[6a,b] were used to measure the binding affinity of ligands to CAII. In the fluorescence method, dansylamide (which has $K_b = 4.0 \times 10^6$ M^{-1} for CAII, determined by a direct fluorescence method[6c] each time before the measurement of other ligands) was allowed to compete against nonfluorescent ligands for CAII. In ACE, a fixed concentration of a charged ligand with known binding constant was allowed to compete with the neutral ligand of interest. The binding constants for the competing ligands were determined by the analysis of the change of electrophoretic mobility of the CAII-charged ligand complex. Values of the binding constants determined by both ACE and fluorescence agreed to within the uncertainty of these measurements (20%).

Measurement of pK_a. The arylsulfonamides were titrated using 1 N NaOH in water; the value of pH in the solution was measured by a glass electrode. The values of pK_a were obtained by performing nonlinear least-squares fits of the values of pH versus volumes of added NaOH; this fit yielded values of pK_a of 10.2, 9.9, 10.1, and 9.8 for the ligands **4A**,**B**,**G**,**H**, respectively (the uncertainty is ±0.2).

Acknowledgment. This work was supported by NIH Grant GM 30367. Mass spectrometry was performed by Dr. A. Tyler and Ms. N. Niedowski. The Harvard University Mass Spectrometry Facility was supported by NSF Grant CHE 90 20042 and NIH Grant 1 S10 RR0671601. We also thank Dr. Hans Biebuyck and Dr. Donovan Chin for helpful discussions.

References

(1) (a) Jain, A.; Whitesides, G. M.; Alexander, R. S.; Christianson, D. W. Identification of Two Hydrophobic Patches in the Active-Site Cavity of Human Carbonic Anhydrase II by Solution-Phase and Solid-State Studies and Their Use in the Development of Tight-Binding Inhibitors. *J. Med. Chem.* **1994**, *37*, 2100–2105. (b) Portoghese, P. S. Bivalent Ligands and the Message-address Concept in the Design of Selective Opioid Receptor Antagonists. *Trends Pharmacol. Sci.* **1989**, *10*, 230–235. (c) Broom, A. D. Rational Design of Enzyme Inhibitors: Multisubstrate Analogue Inhibitors. *J. Med. Chem.* **1989**, *32*, 2–7. (d) Jencks, W. P. On the Attribution and Additivity of Binding Energies. *Proc. Natl. Acad. Sci. U.S.A.* **1981**, *78*, 4046–4050.

(2) (a) Dryjanski, M.; Pratt, R. F. Steady-State Kinetics of the Binding of β-Lactams and Penicilloates to the Second Binding Site of the *Enterobacter cloacae* P99 β-Lactamase. *Biochemistry* **1995**, *34*, 3561–3568. (b) Dryjanski, M.; Pratt, R. F. Inactivation of the *Enterobacter cloacae* P99 β-Lactamase by a Fluorescent Phosphonate: Direct Detection of Ligand Binding at the Second Site. *Biochemistry* **1995**, *34*, 3569–3575. (c) Tsuda, Y.; Cygler, M.; Gibbs, B. F.; Pedyczak, A.; Fethiere, J.; Yue, S. Y.; Konishi, Y. Design of Potent Bivalent Thrombin Inhibitors Based on Hirudin Sequence: Incorporation of Nonsubstrate-type Active Site Inhibitors. *Biochemistry* **1994**, *33*, 14443–14451. (d) Hakansson, K.; Liljas, A. The Structure of a Complex Between Carbonic Anhydrase II and a New Inhibitor, Trifluoromethane Sulfonamide. *FEBS. Lett.* **1994**, *350*, 319–322. (d) Hopfner, K. P.; Ayala, Y.; Szewczuk, Z.; Konishi, Y.; Cera, E. D. Chemical Compensation in Macromolecular Bridge-Binding to Thrombin. *Biochemistry* **1993**, *32*, 2947–2953. (f) Appelt, K. Crystal Structures of HIV-1 Protease-inhibitor Complexes. *Perspect. Drug Dis. Des.* **1993**, *1*, 23–48. (g) Weinhold, E. G.; Knowles, J. R. Design and Evaluation of a Tightly Binding Fluorescent Ligand for Influenza A Hemagglutinin. *J. Am. Chem. Soc.* **1992**, *114*, 9270–9275.

(3) (a) Dodgson, S. J.; Tashian, R. E.; Gros, G.; Carter, N. D. *The Carbonic Anhydrase: Cellular Physiology and Molecular Genetics;* Plenum Press: New York and London, 1991. (b) Pocker, Y.; Sarkanen, S. Carbonic Anhydrase: Structure, Catalytic Versatility, and Inhibition. *Adv. Enzymol. Relat. Areas Biochem.* **1978**, *47*, 149–274.

(4) (a) Liljas, A.; Haakansson, K.; Jonsson, B. H.; Xue, Y. Inhibition and Catalysis of Carbonic Anhydrase. Recent Crystallographic Analyses. *Eur. J. Biochem.* **1994**, *219*, 1–10. (b) Eriksson, A. E.; Liljas, A. Refined Structure of Bovine Carbonic Anhydrase III at 2.0 Å Resolution. *Proteins* **1993**, *16*, 29–42.

(5) (a) Scott, B. T. Topical Carbonic Anhydrase Inhibitors: Potential Adjuvants to Glaucoma Therapy in the Future. *Optom. Vis. Sci.* **1994**, *71*, 332–338. (b) Hiett, J. A. Topical Carbonic Anhydrase Inhibitors: a New Perspective in Glaucoma Therapy. *Optom. Clin.* **1992**, *2*, 97–112. (c) Hurvitz, L. M.; Kaufman, P. L.; Robin, A. L.; Weinreb, R. N.; Crawford, K.; Shaw, B. New Developments in the Drug Treatment of Glaucoma. *Drugs* **1991**, *41*, 514–532.

(6) (a) Avila, L. Z.; Chu, Y.; Blossey, E. C.; Whitesides, G. M. Use of Affinity Capillary Electrophoresis to Determine Kinetic and Equilibrium Constants for Binding of Arylsulfonamides to Bovine Carbonic Anhydrase *J. Med. Chem.* **1993**, *36*, 126–133. (b) Chu, Y.; Avila, L. Z.; Biebuyck, H. A.; Whitesides, G. M. Use of Affinity Capillary Electrophoresis to Measure Binding Constants of Ligands to Proteins. *J. Med. Chem.* **1992**, *35*, 2915–2917. (c) Jain, A.; Huang, S. G.; Whitesides, G. M. The Length of Oligoglycine- and Oligo(ethylene glycol)-Derived *para*- Substituents Has No Effect on the Affinity of Benzenesulfonamides for Carbonic Anhydrase II in Solution. *J. Am. Chem. Soc.* **1994**, *116*, 5057–5062.

(7) (a) Hansch, C. Quantitative Structure-Activity Relationships and the Unnamed Science. *Acc. Chem. Res.* **1993**, *26*, 147–153. (b) Hansch, C.; Klein, T. E. Molecular Graphics and QSAR in the Study of Enzyme-Ligand Interactions. On the Definition of Bioreceptors. *Acc. Chem. Res.* **1986**, *19*, 392–400. (c) Carotti, A.; Raguseo, C.; Campagna, F.; Langridge, R.; Klein, T. E. Inhibition of Carbonic Anhydrase by Substituted Benzenesulfonamides. A Reinvestigation by QSAR and Molecular Graphics Analysis. *Quant. Struct.-Act. Relat.* **1989**, *8*, 1–10. (d) King, R. W.; Burgen, A. S. V. Kinetic Aspects of Structure-Activity Relations: the Binding of Sulfonamides by Carbonic

Anhydrase. *Proc. R. Soc. London, B* **1976**, *193*, 107–125. (d) Chin, D. N.; Whitesides, G. M. Molecular Dynamics Simulations of Bound $H_2NO_2SC_6H_4CONH(Gly)_3COOBn$ to the Active Site of Human Carbonic Anhydrase II. *J. Am. Chem. Soc.*, in press.

(8) (a) Greer, J.; Erickson, J. W.; Baldwin, J. J.; Varney, M. D. Application of the Three-Dimensional Structures of Protein Target Molecules in Structure-Based Drug Design. *J. Med. Chem.* **1994**, *37*, 1035–1054. (b) Sugrue, M. F.; Gautheron, P.; Grove, J.; Mallorga, P.; Vaider, M. P.; Schwam, H.; Baldwin, J. J.; Christy, M. E.; Ponticello, G. S. MK-927: a Topically Active Ocular Hypotensive Carbonic Anhydrase Inhibitor. *J. Ocul. Pharmacol.* **1990**, *6*, 9–22. (c) Baldwin, J. J.; Ponticello, G. S.; Anderson, P. S.; Christy, M. E.; Murcko, M. A.; Randall, W. C.; Schwam, H.; Sugrue, M. F.; Springer, J. P.; Gautheron, P. Thienothiopyran-2-sulfonamides: Novel Topically Active Carbonic Anhydrase Inhibitors for the Treatment of Glaucoma *J. Med. Chem.* **1989**, *32*, 2510–2513.

(9) (a) Cappalonga, A. M.; Alexander, R. S.; Christianson, D. W. Mapping Protein-Peptide Affinity: Binding of Peptidylsulfonamide Inhibitors to Human Carbonic Anhydrase II. *J. Am. Chem. Soc.* **1994**, *116*, 5063–5068. (b) Nair, S. K.; Calderone, T. L.; Christianson, D. W.; Fierke, C. A. Altering the Mouth of a Hydrophobic Pocket. Structure and Kinetics of Human Carbonic Anhydrase II Mutants at Residue Val-121. *J. Biol. Chem.* **1991**, *266*, 17320–17325. (c) Alexander, R. S.; Nair, S. K.; Christianson, D. W. Engineering the Hydrophobic Pocket of Carbonic Anhydrase II. *Biochemistry* **1991**, *30*, 11064–11072.

(10) For monographs, see: (a) Tanford, C. *The Hydrophobic Effect*, 2nd ed.; Wiley: New York, 1980. (b) Ben-Naim, A. *Hydrophobic Interactions*; Plenum: New York, *1980*. For extensive reviews, see: (c) Blokzijl, W.; Engberts, B. F. N. Hydrophobic Effects. Opinions and Facts. *Anges Chem., Int. Ed. Engl.* **1993**, *32*, 1545–1579. (d) Muller, N. Search for a Realistic View of Hydrophobic Effects. *Acc. Chem. Res.* **1990**, *23*, 23–28. (e) Privalov, P. L.; Gill, S. J. The Hydrophobic Effect: a Reappraisal. *Pure Appl. Chem.* **1989**, *61*, 1097–1104. (f) Privalov, P. L.; Gill, S. J. Stability of Protein Structure and Hydrophobic Interaction. *Adv. Protein Chem.* **1988**, *39*, 191–234. (g) Shinoda, K. "Iceberg" Formation and Solubility. *J. Phys. Chem.* **1977**, *81*, 1300–1302. (h) Kauzmann, W. Some Factors in the Interpretation of Protein Denaturation. *Adv. Protein Chem.* **1959**, *14*, 1–63.

(11) (a) Wendell, A. L.; Sauer, R. T. Alternative Packing Arrangements in the Hydrophobic Core of λ Repressor. *Nature* **1989**, *339*, 31–36. (b) Eriksson, A. E.; Baase, W. A.; Zhang, X.; Heinz, D. W.; Blaber, M.; Baldwin, E. P.; Matthews, B. W. Response of a Protein Structure to Cavity-Creating Mutations and its Relation to the Hydrophobic Effect. *Science* **1992**, *255*, 178–183. (c) Matsumura, M.; Becktel, W. J.; Matthews, B. W. Hydrophobic Stabilization in T4 Lysozyme Determined Directly by Multiple Substitutions of Il3 3. *Nature* **1988**, *334*, 406–410.

(12) (a) Jacquemain, D.; Wolf, S. G.; Leveiller, F.; Frolow, F.; Einstein, M.; Lahav, M.; Leiserowitz, L. Correlation between Observed Crystalline Self-Assembly of Fluorocarbon and Hydrocarbon Amphiphiles at the Air-Water Interface and Calculated Lattice Energy. Determination of Electrostatic Properties of the CF_2 Group from a Low-Temperature X-ray Diffraction Study of Perfluoroglutaramide. *J. Am. Chem. Soc.* **1992**, *114*, 9983–9989. (b) Kabalnov, A. S.; Makarov, K. N.; Shcherbakova, O. V. Solubility of Fluorocarbons in Water as a Key Parameter Determining Fluorocarbon Emulsion Stability. *J. Fluorine Chem.* **1990**, *50*, 271–284. (c) Claesson, P. M.; Christenson, H. K. Very Long Range Attractive Forces between Uncharged Hydrocarbon and Fluorocarbon Surfaces in Water. *J. Phys. Chem.* **1988**, *92*, 1650–1655. (d) Mukerjee, P.; Handa, T. Adsorption of Fluorocarbon and Hydrocarbon Surfactants to Air-Water, Hexane-Water, and Perfluorohexane-Water Interfaces. Relative Affinities and Fluorocarbon-Hydrocarbon Nonideality Effects. *J. Phys. Chem.* **1981**, *85*, 2298–2303.

(13) (a) Gordon, A. J.; Ford, R. A. *The Chemist's Companion: a Handbook of Practical Data, Techniques, and References*; John Wiley & Sons, Inc.: New York, 1972; pp 82–87. (b) Weast, R. C.; Lide, D. R.; Astle, M. J.; Beyer, W. H. *CRC Handbook of Chemistry and Physics*, 70th ed.; CRC Press, Inc.: Boca Raton, FL, 1990; p F188. (c) Seebach, D. Organic Synthesis-Where Now? *Angew. Chem., Int. Ed. Engl.* **1990**, *29*, 1320–1367. (d) Claesson, P. M.; Christenson, H. K. Very Long Range Attractive Forces Between Uncharged Hydrocarbon and Fluorocarbon Surfaces in Water. *J. Phys. Chem.* **1988**, *92*, 1650–1655. (e) Israelachvili, J. N. *Intermolecular and Surface Forces*, 2nd ed.; Academic Press: London, 1992; p 315. (f) Battino, R.; Clever, H. L. The Solubility of Gases in Liquids. *Chem. Rev.* **1966**, *66*, 395–463. (g) Weast, R. C.; Lide, D. R.; Astle, M. J.; Beyer, W. H. *CRC Handbook of Chemistry and Physics*, 70th ed.; CRC Press, Inc.: Boca Raton, FL, 1990; pp E75–E76.

(14) (a) Hermann, R. B. *Structure and Reactivity in Aqueous Solution*; Truhlar, Cramer, Eds.; American Chemical Society: Washington, DC, 1994; pp 336–358. (b) Hermann, R. B. Calculation of Hydrophobic Interactions from Molecular Dynamics, Surface Areas, and Experimental Hydrocarbon Solubilities. *J. Comput. Chem.* **1993**, *14*, 741–750. (c) Hermann, R. B. Use of Solvent Cavity Area and Number of Packed Solvent Molecules around a Solute in Regard to Hydrocarbon Solubilities and Hydrophobic Interactions. *Proc. Natl. Acad. Sci. U.S.A.* **1977**, *74*, 4144–4145.

(15) (a) Brinck, T.; Murray, J. S.; Politzer, P. Octanol/water Partition Coefficients Expressed in terms of Solute Molecular Surface Areas and Electrostatic Potentials. *J. Org. Chem.* **1993**, *58*, 7070–7073. (b) De, B. J.; Hermens, J. Relationships between Octanol/water Partition Coefficients and Total Molecular Surface Area and Total Molecular Volume of Hydrophobic Organic Chemicals. *Quant. Struct.-Act. Relat.* **1990**, *9*, 11–21.

(16) Chothia, C. Principles that Determine the Structure of Proteins. *Annu. Rev. Biochem.* **1984**, *53*, 537–572.

(17) Lee, B.; Richards, F. M. The Interpretation of Protein Structures: Estimation of Static Accessibility. *J. Mol. Biol.* **1971**, *55*, 379–400.

(18) Richards, F. M. Areas, Volumes, Packing, and Protein Structure. *Annu. Rev. Biophys. Bioeng.* **1977**, *6*, 151–176.

(19) Hermann, R. B. Theory of Hydrophobic Bonding. II. The Correlation of Hydrocarbon Solubility in Water with Solvent Cavity Surface Area. *J. Phys. Chem.* **1972**, *76*, 2754–2759.

(20) (a) Rees, D. C.; Wolfe, G. M. Macromolecular Solvation Energies Derived from Small Molecule Crystal Morphology. *Protein Sci.* **1993**, *2*, 1882–1889. (b) Tunon, I.; Silla, E.; Pascual, A. J. L. Molecular Surface Area and Hydrophobic Effect. *Protein Eng.* **1992**, *5*, 715–716.

(21) In this and other tables and figures, the compounds are designated by numbers indicating the table in which they are first listed. Thus, compound **2A** is the first compound in Table 2.

(22) The best-fit values in Figures 3–6 were obtained by linear regression analysis using the equation $y = m_0x + m_1$, where m_0 and m_1 are slope and y-intercept, respectively. The values of standard error and regression coefficients were shown after the best-fit values of interest. The probabilities of null hypothesis are below 1% in Figures 3A and 4–6 and above 10% in Figure 3B,C calculated on the basis of a t-distribution with N points. The higher probabilities of null hypothesis in Figure 3B,C indicate that the surface area (x-axis in Figure 3B) or ΔG_P (x-axis in Figure 3C) may not be the only factor that determines the binding affinity; other factors, e.g., the shape or flexibility of the hydrophobic groups, may also contribute to binding.

(23) (a) De Young, L. R.; Dill, K. A. Partitioning of Nonpolar Solutes into Bilayers and Amorphous n-Alkanes. *J. Phys. Chem.* **1990**, *94*, 801–809. (c) Radzicka, A.; Wolfenden, R. Comparing the Polarities of the Amino Acids: Side-Chain Distribution Coefficients between the Vapor Phase, Cyclohexane, Octanol, and Neutral Aqueous Solution. *Biochemistry* **1988**, *27*, 1664–1670. (c) Eisenberg, D.; McLachlan, A. D. Solvation Energy in Protein Folding and Binding. *Nature* **1986**, *319*, 199–203. (d) Chothia, C. The Nature of the Accessible and Buried Surfaces in Proteins. *J. Mol. Biol.* **1976**, *105*, 1–14.

(24) (a) Brooks, B. R.; Bruccoleri, R. E.; Olafson, B. D.; States, D. J.; Swaminathan, S.; Karplus, M. CHARM: A Program for Macromolecular Energy, Minimization, and Dynamics Calculations. *J. Comput. Chem.* **1983**, *4*, 187–217. (b) *QUANTA 3.3 Parameter Handbook*; MSI: Bulington, MA, 1992.

(25) In principle, the concentration of the ligand in octanol can also be measured by UV spectroscopy directly. Since octanol has background absorption (0.5 at wave length 225 nm compared to water), we calculated the concentration of the ligand in octanol as described in the text.

(26) Leo, A.; Hansch, C.; Elkins, D. Partition Coefficients and Their Uses. *Chem. Rev.* **1971**, *71*, 525–616.

JM950114Z